X-Ray photoreduction of a di(μ-oxo)$Mn^{III}Mn^{IV}$ complex occurs at temperatures as low as 20 K†

Lionel Dubois,[ac] Lilian Jacquamet,[b] Jacques Pécaut[c] and Jean-Marc Latour*[a]

Received (in Cambridge, UK) 27th June 2006, Accepted 30th August 2006
First published as an Advance Article on the web 18th September 2006
DOI: 10.1039/b609072a

Full reduction of the $Mn^{III}(\mu\text{-}O)_2Mn^{IV}$ core to $Mn^{II}(\mu\text{-}OH_2)_2Mn^{II}$ is observed upon irradiation by an X-ray beam at *ca.* 20 K.

High energy X-ray beams provided by synchrotrons have allowed a formidable surge in protein crystallography over the past decade. Nevertheless, the use of a high X-ray flux can damage the protein chain through the formation of radicals.[1] Moreover, in the case of metalloproteins containing redox active metals, the metals can be reduced, casting doubt on the exact redox state of the metal core of the structurally characterised protein. Such a problem was recently highlighted[2] for photosystem II where the discrepancy of the various structure determinations was ascribed to different reduction levels of the tetramanganese cluster from the $(Mn^{III})_2$ $(Mn^{IV})_2$ state to Mn^{II}. This effect was exquisitely analysed quantitatively and it was proposed that lowering the data collection temperature from 100 K to 10 K would decrease metal reduction. This prompts us to report our observations that even at 20 K a di(μ-oxo) $Mn^{III}Mn^{IV}$compound can be X-ray reduced, and that the structure of the final compound can be analysed at the molecular level.

In the course of our studies of dimanganese complexes as potential models of the manganese catalases,[3] we were interested in studying the $Mn^{III}(\mu\text{-}O)_2Mn^{III}$ complexes of a series of tripodal ligands based on successive replacement of one pyridine group by a carboxylate from trispicolylamine (tpa) to bispicolylglycine (Hbpg) to picolyldiacetic acid (H_2pda). As a precursor to the complex of the latter ligand, we synthesised the $Mn^{III}(\mu\text{-}O)_2Mn^{IV}$ pda complex **1** which was isolated as its sodium salt: $[(pda)Mn(O)_2Mn(pda)]Na(H_2O)_3\cdot 3(H_2O)$. The X-ray structure of **1**[4] is illustrated in Fig. 1. The Na and O(6) atoms lie on a twofold symmetry axis and the center of the Mn_2O_2 rhombus is a symmetry center, which imposes that the two Mn sites are statistically disordered. The in-plane coordination of each manganese comprises of four ligands: the two oxo bridges, one carboxylato oxygen and the tertiary nitrogen. One carboxylato oxygen and a pyridine nitrogen occupy the axial positions. The short Mn–O_{oxo} and Mn–Mn distances (1.82 Å and 2.67 Å, respectively) are characteristic of the di(μ-oxo)dimanganese(III,IV) core. In addition, this structure revealed that **1** is an infinite chain compound, where molecules of complex are bridged by a triaquasodium cation linked to two in-plane carboxylates.

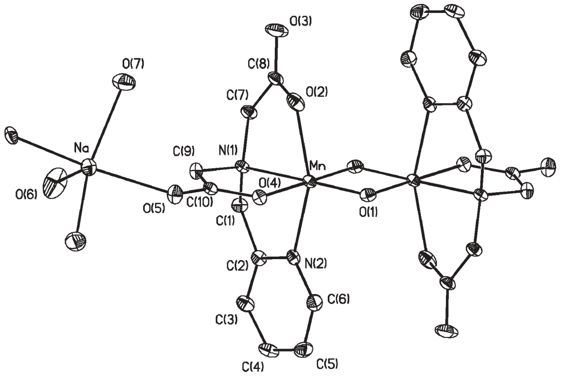

Fig. 1 X-ray structure of compound **1** (Ellipsoids are drawn at 30% probability). Distances in Å: Mn–O(1) 1.809(3), 1.825(3); Mn–N(1) 2.102(4); Mn–N(2) 2.129(4); Mn–O(2) 2.092(4); Mn–O(4) 1.969(3); Mn–Mn 2.6662(13); Mn–O(1)–Mn angle 94.41(14)°.

Compound **1** has been studied by X-ray absorption spectroscopy at 20 K in the solid state. Unexpectedly at such a low temperature, a clear evolution of the spectra was observed, as illustrated in Fig 2 for the pre-edge and XANES regions. This evolution was completed after recording 9 spectra (S1 to S9). Since the recording time amounted to 17 min and 1 min was needed to re-optimise the beam between the spectra, the full experiment required *ca.* 2 h 40 min.

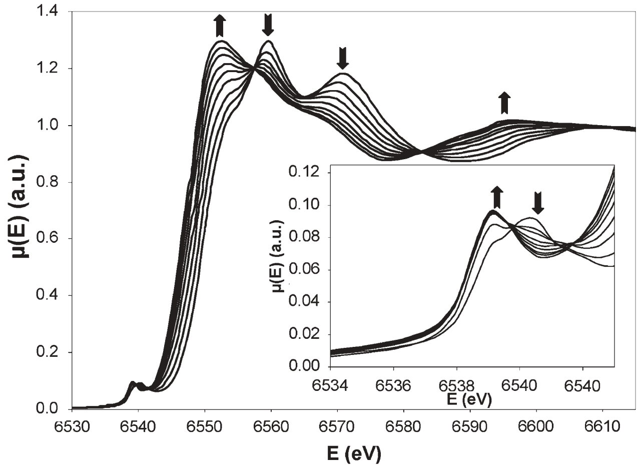

Fig. 2 Successive XANES and pre-edge (inset) spectra of compound **1** recorded at 20 K.

---

[a] *Laboratoire DRDC/PMB, UMR 5155 CEA-CNRS-UJF, CEA-Grenoble, 38054 Grenoble Cedex 9, France. E-mail: Jean-Marc.Latour@cea.fr; Fax: +33 438 78 34 62; Tel: +33 438 78 44 07*
[b] *Laboratoire LCCP, IBS, UMR 5075 CEA-CNRS-UJF, 38027 Grenoble Cedex 1, France*
[c] *Laboratoire LCIB, UMR E, CEA-Grenoble, 38054 Grenoble Cedex 9, France*

† Electronic supplementary information (ESI) available: Preparation, X-ray crystal structure determination and X-ray absorption data collection, treatment and fitting details. See DOI: 10.1039/b609072a

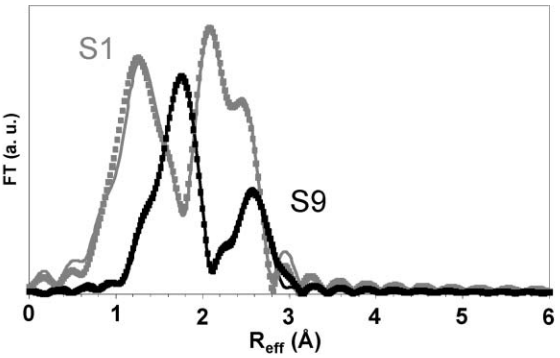

Fig. 3 Initial (S1, grey) and final (S9, black) EXAFS spectra of compound **1** recorded at 20 K. The solid lines are the best fit obtained with the parameters from Table 1.

Fig. 2 illustrates the time evolution of the XANES spectra during irradiation. Spectrum S1 exhibits the characteristic structure of the bis-oxo$Mn^{III}Mn^{IV}$ species with an edge energy of 6549.8 eV.[5,6] The successive spectra shift continuously to lower energy indicating a reduction of the manganese ions' oxidation state. The final spectrum S9 presents a single maximum at an edge energy of 6546.9 eV. The *ca.* 3 eV shift between S1 and S9 is in agreement with the reduction of the Mn_2 core to a $Mn^{II}Mn^{II}$ redox state in the final compound **2**.[7] Two isosbestic points appear at 6557.5 and 6583.0 eV, which indicates that **1** transforms into a single compound.

The S1 pre-edge presents a major peak at 6540.4 eV flanked by two shoulders at 6539.2 and 6542.0 eV, in agreement with a Mn^{III}–Mn^{IV} core. The two features at higher energy regularly loose intensity and eventually vanish upon irradiation. Simultaneously, a peak builds up rapidly at 6539.2 eV corresponding to a Mn^{II} oxidation state.

Fig. 3 depicts the FT EXAFS spectrum of compound **1** (grey curve). This spectrum comprises three main peaks at 1.28, 2.08 and 2.46 Å (uncorrected for phase shift). The first peak corresponds to the $Mn–O_{oxo}$ and Mn–N/O shells. The second peak corresponds to the Mn–Mn shell, while the last one is associated to the outer carbon shell comprising of the α carbons of the various donor atoms. Indeed, the X-ray structure of **1** indicates that six such carbons are present at 2.79–2.92 Å from the Mn ions.

During beam exposure, the Mn coordination shells undergo dramatic modifications. The $Mn–O_{oxo}$ shell decreases after each spectrum and eventually vanishes. Consequently, a new shell appears at 1.68 Å (uncorrected for phase shift) and its intensity increases gradually. Simultaneously, the intensity of the Mn–Mn shell decreases gradually and eventually moves to *ca.* 2.6 Å. These modifications are completed for S9 (Fig. 3, black curve) and the Mn–O and Mn–Mn shells are shifted to longer distances.

Table 1 Results of EXAFS fitting and selected crystal data for **1**, *n* is the number of atoms in the respective shells

	1 (cryst.) *d*/Å	**1** (SAX) *d*/Å, *n*	**2** (SAX) *d*/Å, *n*
$Mn–O_{oxo}$	1.809 1.825	1.83, 2	2.14, 3
Mn–N/O	1.969–2.129	1.98, 4	2.22, 3
Mn–Mn	2.6662	2.65, 1	3.02, 1
$Mn–C_{\alpha}$	2.79–2.92	2.82, 4	3.12, 4

The first and last spectra S1 and S9 have been fitted to obtain structural information. The fit values are listed in Table 1. S1 is best fitted with 2 O at 1.83 Å, 4 N/O at 1.98 Å, 1 Mn at 2.65 Å and 4 C_{α} at 2.82 Å. These EXAFS distances are consistent with a di(μ-oxo)$Mn^{III}Mn^{IV}$ core[5,6] and in perfect agreement with the distances derived from crystallography. Concerning S9, the best fit gives 3 N/O at 2.14 Å, 3 N/O at 2.22 Å, 1 Mn at 3.02 Å and 4 C_{α} at 3.12 Å. The most salient change on going from S1 to S9 is the shift to longer distances of the the Mn–O and Mn–Mn shells: the short $Mn–O_{oxo}$ distance (1.83 Å) in S1 has been replaced by a longer Mn–O distance (2.14 Å), and similarly the short Mn–Mn interaction (2.65 Å) has been replaced by another at longer distance (3.02 Å). Overall the Mn–N/O distances have been elongated by *ca.* 0.27 Å and average 2.18 Å. This elongation is consistent with the reduction of the dimanganese core from $Mn^{III}Mn^{IV}$ to $Mn^{II}Mn^{II}$.[8] As a consequence the Mn–Mn distance has increased by *ca.* 0.37 Å to 3.02 Å. This Mn–Mn distance is still quite short and compatible only with a Mn_2O_2 core. Indeed, examination of the literature reveals that comparable distances have been observed for dinuclear Mn^{II} species only for di(μ-phenoxo)dimanganese(II) complexes possessing an Mn_2O_2 diamond core.[9,10] This strongly suggests that during the reduction the Mn_2O_2 core has been modified but that it is retained. The simple explanation of these observations is thus that protonation of the oxo bridges to hydroxide ions or water molecules has occurred upon reduction of the dimanganese core. In this respect, it is worth noting that, as stated above, **1** is isolated with a triaquasodium counter cation and three water molecules which may constitute a ready proton source. The observed Mn–O distances give additional indication on the nature of the bridging ligand. Indeed, the shortest Mn–ligand distances observed (2.14 Å) appear too long to be associated to hydroxides[11] ($Mn–O_{hydroxide} <$ 2.095 Å) but they are entirely consistent with water ligands[12] ($Mn–O_{water} >$ 2.11 Å). Therefore, the resulting compound can be best described as a di(μ-aqua)$Mn^{II}Mn^{II}$ complex, although a mixed (hydroxo)(aqua) bridging pattern cannot be strictly excluded.

In summary, the present study demonstrates that the di(μ-oxo)$Mn^{III}Mn^{IV}$ core can be rapidly reduced within an X-ray beam even at 20 K and in the solid state. This reduction occurs with protonation of the oxo bridge ion in spite of the fact that water is present in a very limited quantity (*i.e.* 3 molar eq. per oxo bridge). These observations not only support but also re-emphasise the conclusions of Yachandra *et al.*[2] that metal sites in proteins are far more sensitive to reduction than the protein itself to radical damage. In the present case however, this reduction does not lead to the release of an hydrated Mn^{II} species, probably because of the powder state of the sample and the limited number of water molecules available.

Dr. G. Blondin is thanked for stimulating discussions.

Notes and references

1 E. Garman, *Curr. Opin. Struct. Biol.*, 2003, **13**, 545.
2 J. Yano, J. Kern, K. D. Irrgang, M. J. Latimer, U. Bergmann, P. Glatzel, Y. Pushkar, J. Biesiadka, B. Loll, K. Sauer, J. Messinger, A. Zouni and V. K. Yachandra, *Proc. Natl. Acad. Sci. U. S. A.*, 2005, **102**, 12047.
3 L. Dubois, D.-F. Xiang, X.-S. Tan and J.-M. Latour, *Eur. J. Inorg. Chem.*, 2005, 1565.
4 Crystal data for **1**: Empirical formula: C_{20} H_{38} Mn_2 N_4 Na O_{19}; formula weight: 771.41 g $mole^{-1}$; temperature: 298(2) K; wavelength: 0.71073 Å; crystal system: monoclinic; space group: *C2/c*; unit cell dimensions:

a = 18.9552(19) Å, α = 90°; b = 6.7285(7) Å, β = 94.816(2)°; c = 24.535(3) Å, γ = 90°; volume = 3118.2(6) Å^3, Z = 4; absorption coefficient = 0.912 mm^{-1}; reflections collected: 9671; independent reflections: 3730; [R(int) = 0.0629]; final R indices [$I > 2\sigma(I)$]: $R1$ = 0.0803, w$R2$ = 0.2136, R indices (all data) $R1$ = 0.0966, w$R2$ = 0.2242. CCDC 611555. For crystallographic data in CIF or other electronic format see DOI: 10.1039/b609072a.

5 H. Visser, E. Anxolabéhère-Mallart, U. Bergmann, P. Glatzel, J. H. Robblee, S. Cramer, J.-J. Girerd, K. Sauer, M. P. Klein and V. K. Yachandra, *J. Am. Chem. Soc.*, 2001, **123**, 7031.

6 U. Bossek, H. Hummel, T. Weyhermuller, K. Wieghardt, S. Russell, L. v. d. Wolf and U. Kolb, *Angew. Chem., Int. Ed. Engl.*, 1996, **35**, 1552.

7 T. L. Stemmler, T. M. Sossong, J. I. Goldstein, D. E. Ash, T. E. Elgren, D. M. Kurtz and J. E. Penner-Hahn, *Biochemistry*, 1997, **36**, 9847.

8 L. Dubois, D. F. Xiang, X. S. Tan, J. Pécaut, P. Jones, S. Baudron, L. Le Pape, C. Baffert, S. Chardon-Noblat, M. N. Collomb, A. Deronzier and J. M. Latour, *Inorg. Chem.*, 2003, **42**, 750.

9 T. Aono, H. Wada, M. Yonemura, M. Ohba, H. Okawa and D. E. Fenton, *J. Chem. Soc., Dalton Trans.*, 1997, 1527.

10 T. Nagata, Y. Ikawa and M. Maruyama, *J. Chem. Soc., Chem. Commun.*, 1994, 471.

11 M. Delroisse, A. Rabion, F. Chardac, D. Tetard, J. B. Verlhac, L. Fraisse and J. L. Seris, *J. Chem. Soc., Chem. Commun.*, 1995, 949.

12 R. A. Reynolds, W. R. Dunham and D. Coucouvanis, *Inorg. Chem.*, 1998, **37**, 1232.